Available online at www.sciencedirect.com
SCIENCE DIRECT
Journal of Power Sources 156 (2006) 100–107
JOURNAL OF POWER SOURCES
www.elsevier.com/locate/jpowsour

Bond Graph model of a PEM fuel cell

Rémi Saisset*, Guillaume Fontes, Christophe Turpin, Stéphan Astier

Laboratoire d'Electrotechnique et d'Electronique Industrielle (LEEI), UMR CNRS-INPT 5828, 2 rue Camichel, 31071 Toulouse Cedex 7, France

Available online 21 November 2005

Abstract

A fuel cell clearly is a multidisciplinary system. The authors have chosen an original energy approach that they have applied via the Bond Graph formalism. A PEM fuel cell Bond Graph model is proposed and detailed. Its potentialities are then illustrated by studies on the fuel cell dynamic behavior (current harmonic effects, etc.) and system simulations (electricity generating unit based on a PEM fuel cell, etc.).

Keywords: Bond Graph; Energy approach; Modeling; PEM fuel cell; Experimental validation

1. Introduction

Energy approach is unusual to model electrochemical components for both electrical engineering and electrochemistry communities. Energy is however a unifying concept for many fields of physics. The electrochemical components, especially a fuel cell, are naturally multi-disciplinary components rather well-adapted to this approach: chemistry, electrochemistry, thermal and electrical engineering are concerned. The proposed energy approach is applied via the Bond Graph modeling.

The developed model is an intermediary model between local models which solve differential equations, and models "black boxes". The aim of the authors is to keep strong relations with the physical phenomena.

This energy approach has been generalized to other electrochemical components (Li-ion accumulators, lead-acid accumulators, etc.) [7].

First, the authors recall the basis of Bond Graph modeling. Secondly, they describe the developed fuel cell model. They afterwards study the dynamic behavior of a PEM fuel cell. Finally they illustrate some other potential applications of this model too.

2. Energy approach

A fuel cell [3] clearly is a multidisciplinary system. In order to model such a system, the authors have chosen an energy approach. This approach consists in defining and modeling the energy couplings and the energy exchanges within the system. They have applied it via the Bond Graph formalism which is an explicit graphical tool for describing energy exchanges within a system. Allowing a unified representation of the laws of the various fields of physics, Bond Graphs can moreover facilitate multidisciplinary exchanges.

2.1. Bond Graph principles

In Bond Graphs [1], the energy exchanges within a system are described by bonds which represent the power exchanges. Two variables, effort and flow, are associated with each bond (Fig. 2). These factors have different interpretations in the different fields of physics (Table 1). The product of these two variables is the transferred power. The bond is arbitrarily oriented by a half arrow which indicates the positive power flow orientation. Furthermore, causality is a fundamental concept in Bond Graphs: it defines the cause-effect relations. The causal bar indicates the effort direction (Fig. 2).

2.2. Bond Graph standard elements

Only a limited number of elements are necessary to describe the majority of systems. Table 2 gives these main elements: dissipative element R, inertial element I and storage element C. The connections between these elements are implemented through junctions. There are two types of junctions (Table 3): 1-junctions and 0-junctions which respectively correspond to series connections and parallel connections. They express in fact

* Corresponding author.
E-mail address: name@leei.enseeiht.fr (R. Saisset).

0378-7753/$ – see front matter © 2005 Published by Elsevier B.V.
doi:10.1016/j.jpowsour.2005.08.040

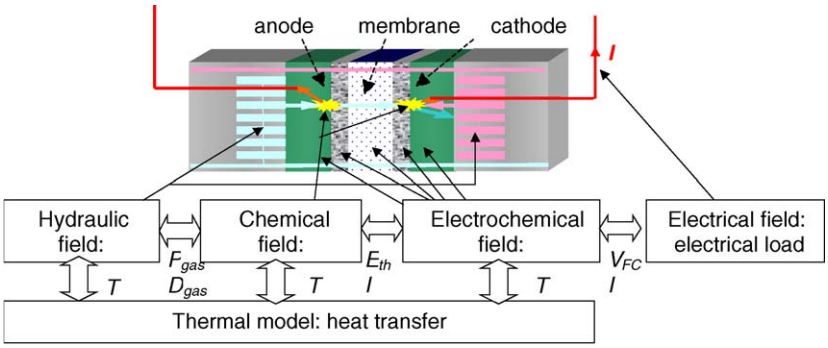

Fig. 1. Representation of a bond.

Table 1
Examples of effort and flow

System	*e*: Effort (unit)	*f*: Flow (unit)
Electrical	*v*: Voltage (V)	*i*: Current (A)
Mechanical	*F*: Force (N)	*V*: Velocity ($m\,s^{-1}$)
Chemical	μ: Chemical potential ($J\,mol^{-1}$)	d*n*/d*t*: Molar flow ($mol\,s^{-1}$)
Hydraulic	*P*: Pressure (N)	d*q*/d*t*: Volume flow ($m^3\,s^{-1}$)
Thermal	*T*: Temperature (K)	d*s*/d*t*: Entropy flow ($J\,K^{-1}\,s^{-1}$)

Table 2
Bond Graph elements

Element	Represents	Equation without causality
R:*r*	Resistance	$e - rf = 0$
I:*i*	Inertia	$e - i\frac{df}{dt} = 0$
C:*c*	Capacitance	$f - c\frac{de}{dt} = 0$
S_e	Effort source	$e = cst$
MS_e	Modulated effort source	$e = e$(input)
S_f	Flow source	$f = cst$
MS_f	Modulated flow source	$f = f$(input)

the generalized Kirchoff's laws. The transformers and the gyrators are used to go from a field of physics to another.

Causal rules exist at the junctions. Only one port can fix the flow through a 1-junction. Only one port can fix the effort at a 0-junction. For instance, an effort source connected to a 0-junction fixes the effort at the junction; the rest of the system fixes the flows through this junction.

3. Bond Graph model of a PEM fuel cell

A global scheme in Fig. 1 presents the different fields which have been modeled, and the main variables of the model. Each

Table 3
Bond Graph junctions

Junction	Represents	Equation
1	Equality of flows	$\sum_i e_i = 0$
0	Equality of effort	$\sum_i f_i = 0$
TF	Transformer	$e_1 = re_2,\ f_2 = rf_1$
GY	Gyrator	$e_1 = rf_2,\ e_2 = rf_1$

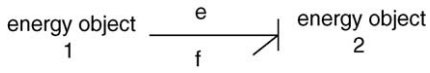

Fig. 2. Description of the different fields of physics in a PEM fuel cell.

field of physics has been represented by a block.

- P_{gas} represents the gas pressures (P_{H_2}, P_{O_2}).
- D_{gas} represents the gas volume flows (D_{H_2}, D_{O_2}).
- E_{th} is the theoretical thermodynamic potential.
- I is the load current.
- V_{FC} is the fuel cell voltage.
- T is the fuel cell temperature.

3.1. Main assumptions

The main assumptions are as follows:

(i) one-dimensional modeling;
(ii) the electrodes are separately modeled;
(iii) the input gases are pure O_2 and pure H_2;
(iv) uniform gas concentration in the supply channels and no pressure losses (entry and exit cell pressures are constant and equal);
(v) the gas diffusion is solved in steady state;
(vi) no parasitic reaction;
(vii) the following state parameters (P, hydration) are known and considered as constant (the hydration level time-constant is very low compared to the studied phenomenon).

3.2. Hydraulic field

In this field, the efforts are the gas pressures P_{gas} in bars, and the flows are the gas volume flows D_{gas} ($m^3\,s^{-1}$). The gas pressures are entry parameters of the model. No losses are considered in the supply channels. The gas volume flows are calculated starting from the gas molar flow J_{igas} ($mol\,s^{-1}$) and the molar volume ($m^3\,mol^{-1}$):

$$D_{gas} = V_m J_{igas} \quad (1)$$

$$V_m = \frac{RT}{10^5 P_{gas}} \quad (2)$$

where R is the perfect gas constant.

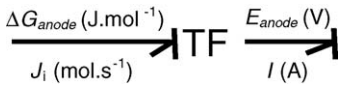

Fig. 3. Calculation of E_{th} at the anode

3.3. Chemical field

This part determines the theoretical thermodynamic potential E_{th}, which represents the conversion of chemical energy to electrical energy. It is equal to the difference between the cathodic and anodic potentials:

$$E_{th} = E_{cathode} - E_{anode} \tag{3}$$

The exit of the chemical block is an effort (Fig. 4): the thermodynamic potential, which results from the free Gibbs energy ΔG at each electrode. The electrical circuit imposes the molar flow to this chemical block. These transformations can be calculated by the relations:

$$E_{anode} = \frac{\Delta G_{anode}}{nF}, \qquad E_{cathode} = -\frac{\Delta G_{cathode}}{nF} \tag{4}$$

$$I = nFJ_i \tag{5}$$

where n is the exchanged electron mole number and F is the Faraday constant. The sign difference in (4) depends on the reaction nature: an oxidation at the anode and a reduction at the cathode.

The transition between the chemical field and the electrochemical field is realized thanks to a transformer, as shown in Fig. 3. The example of the anode is given. The transformer ratio is $1/nF$ as the Eqs. (4) and (5) demonstrate it.

3.3.1. Free Gibbs energy and dependence on gas pressures

The free Gibbs energy variations are calculated from the standard free enthalpy variation of each gas (H_2 for the anode, O_2 for the cathode) at a standard reference pressure. They are corrected by a term taking into account the pressure effect. It represents the Nernst law:

$$\Delta G_{cathode} = \Delta G^{\circ}_{cathode} - \frac{RT}{2}\ln(P_{O_2}),$$
$$\Delta G_{anode} = \Delta G^{\circ}_{anode} - RT\ln(P_{H_2}) \tag{6}$$

3.3.2. Standard free Gibbs energy variation calculations

The theoretical recoverable energy is the enthalpy variation ΔH of the chemical reaction. Unfortunately, the practical recoverable energy, which can be transformed into electrical energy, is the standard free enthalpy variation (standard free Gibbs energy) given by the following relation:

$$\Delta G^{\circ} = \Delta H^{\circ} - T\,\Delta S^{\circ} \tag{7}$$

where ΔS° is the entropy variation (J mol^{-1} K^{-1}) and $T\Delta S^{\circ}$ represents the lost thermal energy (J mol^{-1}), which is often called reaction heat.

The enthalpy and entropy variations represent differences between a start state and a final state of the chemical reactions. They are both calculated for each electrode thanks to this kind of relation:

$$\Delta H^{\circ}_{reaction} = \Delta H^{\circ}_{products} - \Delta H^{\circ}_{reactive\ agents} \tag{8}$$

Enthalpy and entropy variations of a gas are temperature functions:

$$\Delta H^{\circ}(T) = \Delta H^{\circ}(T_0) + \int_{T_0}^{T} \Delta C_p\, d\theta \tag{9}$$

$$\Delta S^{\circ}(T) = \Delta S^{\circ}(T_0) + \int_{T_0}^{T} \left(\frac{\Delta C_p}{\theta}\, d\theta\right) \tag{10}$$

where:

$$C_p = \alpha + \beta\theta + \gamma\theta^2 \tag{11}$$

where θ is the fuel cell temperature and α, β, γ are coefficients which depend on the gas.

It is important to note that the power is not conserved between the entry and the exit of this chemical block (Fig. 4): $P_{gas}D_{gas} \neq \Delta H_{gas}J_{igas}$. Indeed, the chemical energy transported by the gas is not taken into account in the hydraulic power. That is why all these calculations are realized in the block called "thermochemical" in Fig. 4. Today, this is not satisfactory because that does not correspond to the Bond Graph spirit. That illustrates the difficulty for uncoupling the thermochemical phenomena.

3.3.3. Produced reaction heat

The reaction heat is transferred to the thermal model as a thermal power ("pseudo" Bond Graph), which is expressed in Watt (Fig. 4). The temperature calculated in the thermal model is injected into the chemical block, in order to calculate free Gibbs energy variations.

Note: The "pure" Bond Graph modeling would handle temperature and entropy flow. The consequence would be that the used elements R would not be homogeneous to the classical thermal resistances. Because of this difficulty, the Bond Graph users handle classically the "pseudo" Bond Graph where temperature is the effort and the thermal power the "pseudo" flow. The product "temperature by thermal power" is then not homogeneous to a power.

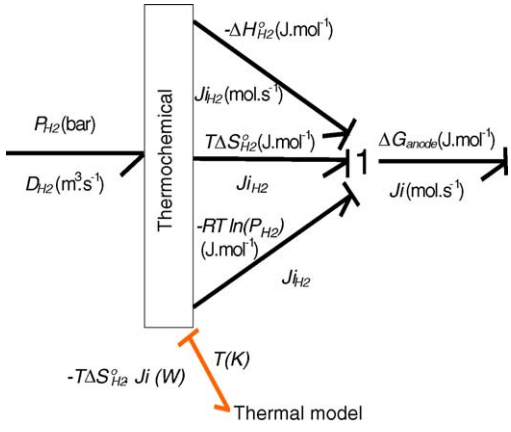

Fig. 4. Chemical field; calculation of ΔG at the anode ($J_{iH_2} = J_i$).

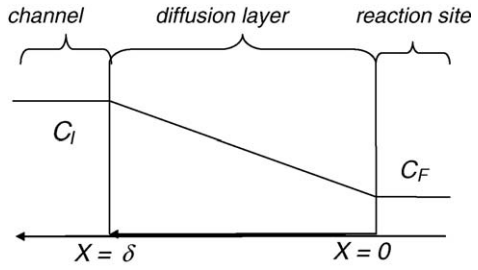

Fig. 5. Gas diffusion.

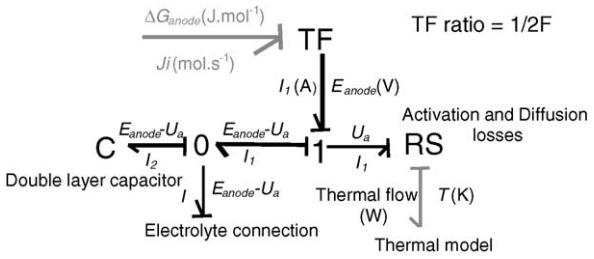

Fig. 6. Electrochemical field at the anode.

3.4. Electrochemical field

The theoretical potential E_{th} is the fuel cell potential when the load current is zero. Unfortunately, this potential strongly decreases when the fuel cell operates. Different losses appear: activation, ohmic and diffusion phenomena. These losses are usually modeled by voltage drops (overvoltages).

3.4.1. Activation losses

At each electrode appear losses generated by the reaction kinetics [5]. These are called activation losses and generate an overvoltage η_{act} which is subtracted to the theoretical electrode potential. A non-linear relation between this overvoltage $\eta_{act,\,a\,or\,c}$ and the electrode current $I_{electrode}$ is given by the Butler–Volmer equation, if the diffusion phenomena are neglected. This law is for example at the anode:

$$I_{anode} = I_{0,a}\, e^{\alpha_{0,a} n_a F \eta_{act,a}/RT} - I_{0,a}\, e^{-(1-\alpha_{0,a}) n_a F \eta_{act,a}/RT} \quad (12)$$

where $I_{0,a}$ is the anode exchange current (A), $\alpha_{0,a}$ is the transfer coefficient of the oxidation reaction, n_a is the exchanged electron mole number and $\eta_{act,\,a}$ is the anodic overvoltage referenced to the anode potential (V).

This equation describes both the oxidation and reduction reactions that take place at one electrode. Naturally, a reaction is predominant at each electrode: oxidation at the anode and reduction at the cathode. The classical Tafel equation can be obtained with these assumptions.

3.4.2. Diffusion losses

Before reaching the reaction sites, the gas goes through a porous layer, called diffusion layer (Fig. 5). The diffusion losses will be higher at the cathode because this electrode is the place of the water production. This phenomenon can be characterized by the Fick's law, which is solved here in steady state:

$$D_f \frac{\partial^2 c}{\partial x^2} = \frac{\partial c}{\partial t} = 0 \quad (13)$$

where D_f is the gas diffusion coefficient through water (m^2 s^{-1}). The final concentration at the reaction site is:

$$C_F = C_I - \frac{J_i \delta}{A D_f} = C_I - \frac{I}{nFA}\frac{\delta}{D_f} \quad (14)$$

where δ is the diffusion layer width (m) and A the cell area (m^2). A limit current I_{lim} can be defined from this expression when the concentration C_F reaches the value 0:

$$I_{lim} = \frac{(C_I A) n F D_f}{\delta} \quad (15)$$

The gas concentrations have a great influence on the exchange current of Butler–Volmer equation (12). The influence of gas diffusion can be included into this equation for example at the cathode [7]:

$$I_{cathode} = \frac{\exp(((1-\alpha_{0,c}) n_c F/RT)\eta_{act,c}) - \exp(-(\alpha_{0,c} n_c F/RT)\eta_{act,c})}{1/I_{0,c} + 1/I_{lim\ Ox,c}\exp((((1-\alpha_{0,c}) n_c F)/RT)\eta_{act,c}) + (1/I_{lim\ Red,c})\exp(-(\alpha_{0,c} n_c F/RT)\eta_{act,c})} \quad (16)$$

where $I_{lim\,Ox,c}$ and $I_{lim\,Red,c}$ are the limit currents defined when the gas concentration at the reaction site reaches the value 0.

3.4.3. Modeling of the activation and diffusion losses

The activation and diffusion losses are modeled by a same nonlinear dissipative element R (Fig. 6). The relation which links the effort to the flow in the Bond Graph is given, for example, by (16) for the cathode. The associated losses represent a thermal power which is injected into the thermal model (Fig. 6).

3.4.4. Double layer capacitors

At each interface electrode/electrolyte appears the double layer phenomenon [2]. Indeed, no charge carrier transfer theoretically exists at this interface. The distance between the species being very short, a capacitor of a great value (several hundreds of mF in our case) is created. A constant element C is used to model this phenomenon (Fig. 6). This double layer capacitor fixes the dynamics of the activation phenomena.

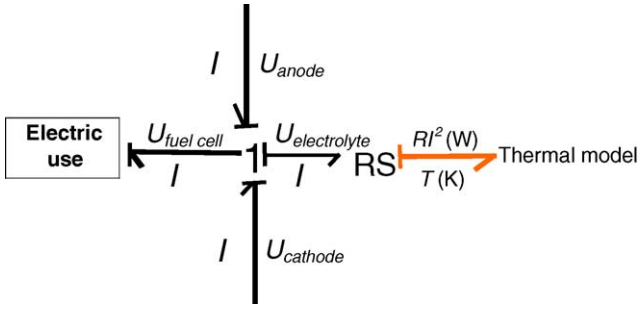

Fig. 7. Connection of the two electrodes.

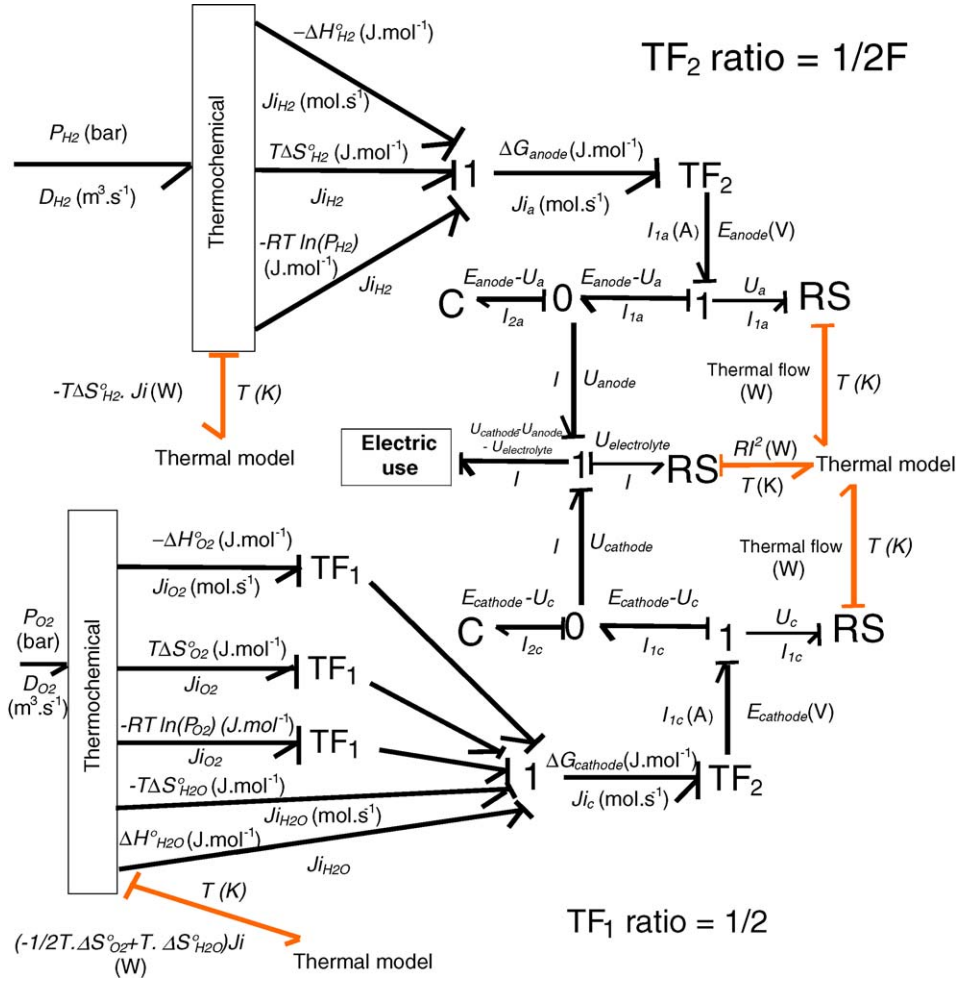

Fig. 8. Global Bond Graph of a PEM fuel cell.

3.4.5. Ohmic losses

The ohmic losses include all the losses in conductors (electrolyte and electrodes) and connections. The main losses being a priori in the electrolyte (membrane), the others are not taken into account in our model.

A linear dissipative element R is used to model these losses (Fig. 7), whose conductivity depends on the membrane material.

For a membrane in Nafion® 117, the protonic conductivity is given by an empirical formula [4]:

$$\sigma = (0.005139\lambda_m - 0.00326)\, e^{(1267((1/303)-(1/T)))} \quad (17)$$

where λ_m is the hydration level.

The hydration level is determined experimentally from a measurement of the membrane resistance (impedance spectroscopy in our case) and geometric data (membrane area and thickness).

The associated losses represent a thermal power which must be injected into the thermal model, like the activation and diffusion losses.

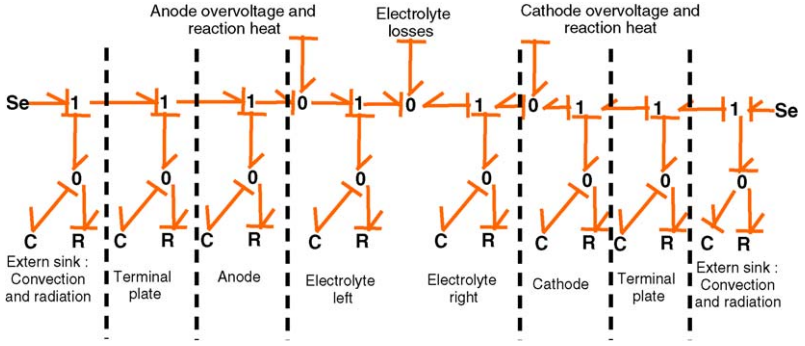

Fig. 9. Thermal Bond Graph of an elementary PEM fuel cell.

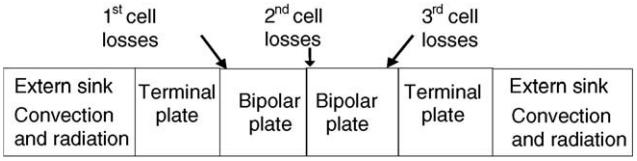

Fig. 10. Thermal model principle for a three-cell association.

The two models of the electrodes are linked on the level of the membrane resistance (Fig. 7). The global model is symmetric (Fig. 8).

3.4.6. Thermal field

Thermal phenomena are very important in a fuel cell. In a first approach, two thermal flow directions are considered: longitudinal and transversal. The fuel stack is modeled as several layers. Each layer is modeled by a *RC* element as shown in Fig. 9. The electrolyte has been divided into two parts in order to keep symmetry, and the losses are injected in the middle. Ambient temperature is imposed by an effort source S_e on both sides of the fuel cell. Activation, diffusion, and all the ohmic losses are the thermal flows.

In a second approach, only the bipolar and terminal plates are considered: the electrolyte thickness (around 200 μm) is much thinner than the bipolar (or terminal) plate (around 1 cm). The thermal model is then simplified (Fig. 10).

The external cooling (fans in our case) is taken into account by modifying the convection coefficient (natural convection: $5\,W\,m^{-2}\,K^{-1}$; forced convection: $50\,W\,m^{-2}\,K^{-1}$). The forced convection coefficient is identified experimentally.

The fuel cell temperature is determined during the model simulation.

4. Parameter identification

The authors are mainly interested in modeling PEM fuel cell stacks. Within a stack, more or less important disparities exist between the different cells [6,7]. It is then assumed that a *n*-cell stack is *n* times the behavior of the equivalent mean cell [8].

The proposed model is a model with dissociated electrodes. Practically, and particularly in the case of a fuel cell stack, only the combined contribution of the two electrodes is measurable. The authors have developed a method to separate the electrodes which will be presented in a future paper.

The membrane resistance is first obtained from an impedance spectroscopy [2,5]. The impedance spectroscopy gives the value of the double layer capacitor too [7,8]. Electrochemical parameters (activation and diffusion) are then identified starting from a curve $V(I)$ [7,8]. The thermal model parameters are identified through thermal measurements and calculations (Fig. 11) [7].

5. Experimental and simulation work

The studied fuel cell is a commercially available 200 W stack composed of 20 cells (Electrochem Inc.). Each cell has an active area of 50 cm^2. The membrane material is Nafion® 117. It is fan-cooled [8].

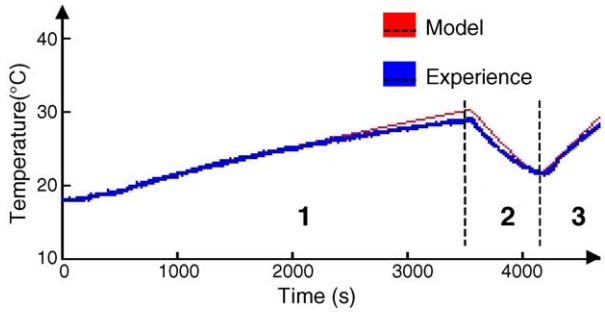

Fig. 11. Thermal measurements and simulations (1 and 3: natural cooling; 2: fan-cooling).

The Electrochem stack has been strongly exploited in our studies [7–9], particularly about the interactions between the fuel cells and the static converters. Moreover, the design of a 200 W electricity generating unit has been studied by associating this fuel cell with a storage device [10]. Some results are illustrated here.

The software 20-sim was used for all simulations. It is dedicated to the Bond Graph simulation. Its use is rather simple and direct.

5.1. Dynamic generation of a voltage–current curve

A curve $V(I)$ is plotted via low frequency sinusoidal current sweeps. This method is in fact a dynamic measurement. The obtained curve is not the "static" curve. Dynamic phenomena are thus solicited according to the sweep frequency. For example, a "hysteresis" phenomenon was observed for low currents with a sweeping frequency around 1 Hz (Fig. 12). The interactions between the activation losses and the double layer capacitors are responsible for this hysteresis. The behavior of the proposed model is good.

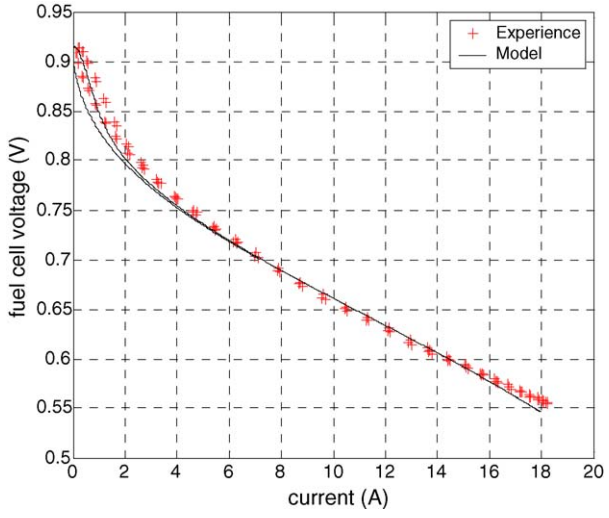

Fig. 12. Experimental and simulation curves $V(I)$ in the case of a sinusoidal current sweep (1 Hz).

5.2. Effects of high current ripples

A sinusoidal current around an operating point is imposed to the fuel cell. In these experiments, the operating point is $I_{DC} = 10$ A, the current amplitude Δi is 3 A peak to peak. Three experimental curves are presented for three different frequencies: 1 Hz, 100 Hz and 10 kHz (Fig. 13).

A hysteresis appears around 100 Hz due to the interactions between the activation losses and the double layer capacitor (Fig. 13b).

This effect does not occur around 1 Hz, because the capacitor has time to charge and to discharge fully (Fig. 13a). In the previous part, a hysteresis appeared at 1 Hz, but the range of the swept currents was higher than in this case; and particularly the low currents are not swept here.

No effect is observed around 10 kHz, because the capacitor can be charged or discharged: the voltage across the capacitor is constant (Fig. 13c). In other words, all current harmonics go through the double layer capacitor (very good filtering). The voltage ripple is only due to the membrane resistance. In each case, the Bond Graph model matches well the experimental results.

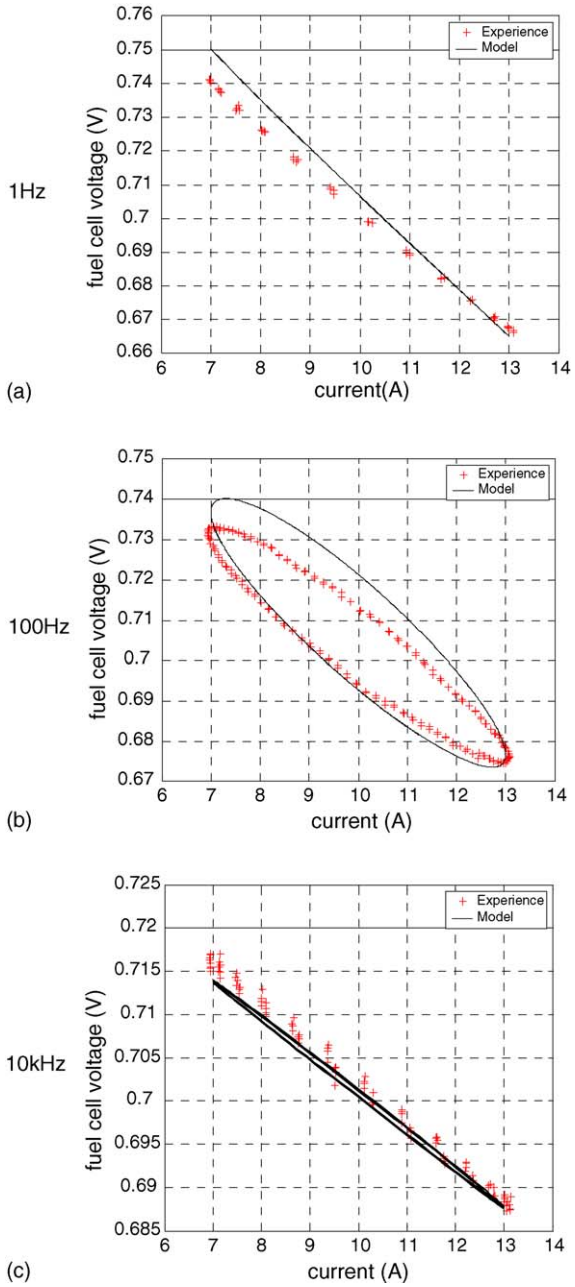

Fig. 13. Model behavior with high current ripples.

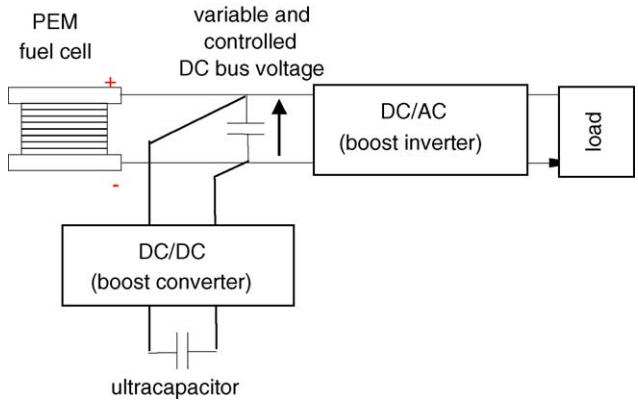

Fig. 14. Example of a studied electricity generating unit.

5.3. Simulation application

The first simulation application was the study of a low power electricity generating unit delivering a standardized single-phase voltage based on a 200 W PEM fuel cell (Fig. 14) [10]. Hybridization between a fuel cell and an ultracapacitor was chosen. The idea was to smooth the power delivered by the fuel cell thanks to the device storage. Originality was the control of the fuel cell operating point: the fuel cell voltage was imposed by the boost converter associated to the ultracapacitor (voltage piloting). Fig. 15 illustrates the behavior of the fuel cell Bond Graph model when a load step occurs. The ultracapacitor supplies the peak power. After the load step, the fuel cell recharges the ultracapacitor.

Moreover, the authors have imagined other electrical piloting types for a fuel cell (current piloting, power piloting). They have validated them thanks to the fuel cell Bond Graph model [7,10].

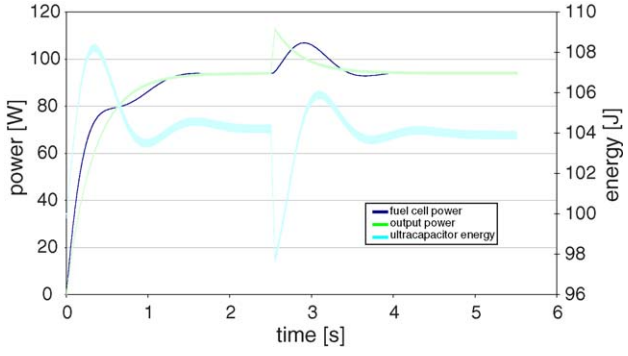

Fig. 15. Simulation of a load step from 95 to 235 W during 50 ms—filtered powers and energy.

Finally, series/parallel associations of fuel cells have been studied thanks to this model [6,7].

6. Conclusion

The energy approach does not propose a local description of the physical phenomena but a global description of their impact. This model has been realized in order to be included in electrical systems. The authors have however demonstrated in the last part that the dynamic behavior of a fuel cell can be finely studied by this approach.

Acknowledgment

The authors would like to thank B. Lafage and M. Comtat from the Laboratoire Genie Chimique (LGC), Toulouse, France.

References

[1] D. Karnopp, R. Rosenberg, Systems Dynamics: A Unified Approach, John Wiley & Sons, 1991.
[2] B.E. Conway, Electrochemical Supercondensators—Scientitfic Fundamentals and Technological Applications, Kluwer Academic/Plenum Publishers, 1999.
[3] J. Larminie, A. Dicks, Fuel Cell Systems Explained, John Wiley & Sons, 2000.
[4] T. Mennola, "Design and experimental characterization of polymer electrolyte membrane fuel cells", Thesis for the Degree of Licentiate of Technology, Finlande, November 2000.
[5] J.P. Diard, B. Le Gorrec, C. Montella, Cinétique Électrochimique. Hermann-Editeurs des sciences et des arts, 1996.
[6] R. Saïsset, C. Turpin, S. Astier, B. Lafage, Proceedings of the IEEE PESC'02 on Study of Thermal Imbalances in Arrangements of Solid Oxide Fuel Cells by means of Bond Graph Modelling, Cairns, Australia, June 2002.
[7] R. Saïsset, "Contribution à l'étude systémique de dispositifs énergétiques à composants électrochimiques—Formalisme Bond Graph appliqué aux piles à combustible, accumulateurs Lithium-ions, véhicule solaire", PhD Thesis of the INP Toulouse, Avril 2004.
[8] G. Fontes, C. Turpin, R. Saïsset, T. Meynard, S. Astier, Proceedings of the IEEE PESC'04 on Interactions between Fuel Cells and Power Converters, Aachen, Germany, June 2004.
[9] G. Fontes, R. Saïsset, C. Turpin, S. Astier, B. Lafage, Proceedings of the IMAACA'04 on Bond Graph Model of a PEM Fuel Cell, Genoa, Italy, October 2004.
[10] R. Saïsset, C. Turpin, S. Astier, J.M. Blaquière, Proceedings of the IEEE VPP'04 on Electricity Generation Starting from a Fuel Cell Hybridised with a Storage Device, Paris, France, October 2004.